Oxygen diffusion into polystyrene–bentonite films

Şaziye Uğur [a,*], Önder Yargı [a], Önder Pekcan [b]

[a] Istanbul Technical University, Department of Physics, 34469 Maslak, Istanbul, Turkey
[b] Kadir Has University 34230, Cibali, Istanbul, Turkey

ARTICLE INFO

ABSTRACT

A simple fluorescence technique is proposed for the measurement of the diffusion coefficient of oxygen into polystyrene–clay composite films. The composite films were prepared from the mixture of surfactant-free pyrene (P)-labeled polystyrene latexes (PS) and modified bentonite (MNaLB) at various compositions at room temperature. These films were annealed at 200 °C above the glass transition (T_g) temperature of polystyrene for 10 min. Oxygen diffusion into the films was monitored with steady state fluorescence (SSF) measurements. Measurements were performed at room temperature for different film compositions (0, 5, 10, 20, 30, 50 and 60 mass% modified bentonite) films to evaluate the effect of MNaLB content on oxygen diffusion. The diffusion coefficient, D of oxygen was determined by the fluorescence quenching method by assuming Fickian transport and increased from 7.4×10^{-10} to 26.9×10^{-10} cm^2 s^{-1} with increasing MNaLB content. This increase in D value was explained by formation of microvoids in the film. These voids are large enough to contribute to the penetration of oxygen molecules through the films. The montmorillonite content did not affect the quenching rate constant, k_q and mutual diffusion coefficient, D_m values.

© 2008 Elsevier B.V. All rights reserved.

1. Introduction

In last decade, there has been growing interest in producing new materials by filling polymers with inorganic natural and/or synthetic compounds (Friedlander and Grink, 1964; Kato et al., 1981; Vaia et al., 1996; Doh and Cho, 1998; Noh and Lee, 1999). These composite materials show high heat resistance, mechanical strength and impact resistance or present weak electrical conductivity and low permeability for gases like oxygen or water vapor. Typically, inorganic fillers like talc, mica, chalk, smectite and bentonite we used. In recent years, polymer/clay (P/C) nanocomposites have become increasingly important because they combine the structural, physical and chemical properties of both the clay mineral and polymer (Uğur et al., 2005, 2006). The clay mineral modifies different properties of the polymer, such as absorbancy, ion exchange capabilities, and thermal and solvent resistance. They improved mechanical properties, gas barrier properties and decreased flammability relative to the simple polymers (Li et al., 2003). The improved composites are widely used in areas such as construction, electronics, consumer products, and transportation (Salahuddin and Akelah, 2002).

The most commonly used clay mineral for the preparation of composites is montmorillonite (Liu and Wu, 2001). The dispersion of montmorillonite particles in polymers can occur as: 1–conventional composite: the filler particles are agglomerated, causing stress concentration and hence reducing the mechanical performance. 2–intercalated nanocomposite: polymer molecules are inserted between individual silicate layers. 3–delaminated (exfoliated nanocomposite): the silicate layers are no longer in close contact to interact with each other and are fully dispersed in the matrix (Gilman, 1999). The last two types of composites show much better mechanical, thermal and barrier properties (Ray and Okamoto, 2003).

The enhancement in barrier properties in composites depends on several factors, such as the amount, length and width of the filler, orientation and dispersion of the filler particles. Gorrasi et al. (2003) studied the transport properties of *n*-pentane and dichloromethane vapours in polypropylene–organophilic clay minerals. The permeability of both solvent vapours was reduced, mainly due to reduced diffusion, since the solubility was less affected by the presence of fillers. Lu et al. (2001a,b) examined the influence of 10 nm diameter silica particles on oxygen diffusion in PDMS polymer film. The oxygen diffusion coefficient decreased increasing silica content. This reduction in D was attributed to tortuous paths towards diffusing gas molecules and reduced molecular mobility of polymer chains caused by the filler particles. Bharadwaj (2001) addressed the modelling of gas barrier properties in polymer–clay mineral nanocomposites based on a similar model. The reduction of permeability arises from the longer diffusive path that the penetrants must travel in the presence of the layered silicate. Recently, Lu and Mai (2005) developed a simple renormalization group model to assess the influence of geometric factors of clay mineral fillers on the gas barrier properties of polymer–clay nanocomposites. Both studies showed that the aspect ratio of exfoliated silicate platelets plays a critical role in controlling the microstructure of polymer–clay nanocomposites and their gas barrier performances. Villaluenga et al. (2007) investigated the permeability, diffusivity and solubility of helium, oxygen and nitrogen into the

---

* Corresponding author. Tel.: +90 212 2856603; fax: +90 212 2856386.
E-mail address: saziye@itu.edu.tr (Ş. Uğur).

Table 1
Particle size frequency distribution of Na-bentonite (P_{NaLB}) and modified bentonite (P_{MNaLB}) with size R

R (μm)	P_{NaLB} (%)	P_{MNaLB} (%)
50	0	–
40	13.5	–
30	22.8	–
20	33.3	–
10	49.8	–
8	51.2	4
6	51.2	12.5
5	53.6	15.6
4	56.4	17.9
3	59.1	22.3
2	63	32.7
1	69.9	56.2
0.8	72.2	63.6
0.6	75.4	71.1
0.5	–	75.2
0.4	–	79.8

R; diameter of particles.

unfilled and filled polypropylene (PP) membranes with montmorillonite using X-ray diffraction, thermogravimetric analyzer, tensile testing and differential scanning calorimetry. The filled membranes exhibited lower gas permeability compared to the unfilled PP membrane and both diffusivity and solubility were reduced by the presence of fillers. This reduction was interpreted in terms of decrease in available free volume in the polymer providing less adsorption sites for gas molecules.

The usual procedure used to measure the diffusion coefficients of gases through a polymeric system is based upon measurements of the amount of gas which permeates a given area of polymer in a given time. Indirect methods are based on the quenching or bleaching action of these gases on the molecular probes imbedded uniformly in the polymer. Several spectroscopic techniques that utilize oxygen quenching to determine the rate of oxygen diffusion through polymer films have been reported. The diffusion coefficient of oxygen into poly (methyl methacrylate) (PMMA) was determined by the quenching of phosphorescence of phenanthrene added into polymer (Shaw, 1967). Barker has used the bleaching action of oxygen on color centers produced by electron beam irradiation of polycarbonate and PMMA by following optically the moving boundary (Barker, 1962). The quenching of fluorescence of naphthalene in PMMA was studied by oxygen in thin films after displacement of nitrogen atmosphere over the sample by oxygen (MacCallum and Rudkin, 1978). Cox and Dunn (1986a,b), MacCallum and Rudkin (1978) measured oxygen diffusion coefficient by fluorescence quenching in planar sheets of poly(dimethyl siloxane) (Cox and Dunn, 1986a,b), filled poly(dimethyl siloxane) sample (Cox and Dunn, 1986a,b) and polystyrene (MacCallum and Rudkin, 1978). They monitored oxygen quenching of a fluorophore as a function of time by assuming that fluorophore dispersed homogeneously within the films. The mathematical determination of D varied, but a single underlying assumption in all cases was that the time-dependent emission intensity was measured during the experiment. In some cases, the intensity versus time curve was converted to a concentration versus time curve using the Stern–Volmer relationship (Cox and Dunn, 1986a,b). Winnik and Manners (Jayarajah et al., 2000; Ruffolo et al., 2000; Lu et al., 2001a,b) have used time-scan experiments to measure the decay of luminescence intensity as oxygen diffuses into polymer films under constant illumination and the growth of intensity as oxygen diffuses out of the film. They interpreted their data with the aid of theoretical expressions based on Stern–Volmer quenching kinetics with Fick's laws of diffusion. In some of our earlier studies, we examined the effect of annealing (Pekcan and Ugur, 1999) and packing (Pekcan and Ugur, 2000) on the oxygen diffusion coefficient, D, in poly(methyl methacrylate) by using steady state (SSF) and photon transmission (PT) techniques. While the D values increased

by increasing the film thickness (packing) (Pekcan and Ugur, 2000), no temperature effect (Pekcan and Ugur, 1999) was observed on the diffusion coefficient, D.

In this contribution, we report oxygen diffusion into PS/montmorillonite composite films containing various amounts of montmorillonite by using fluorescence quenching. A model was developed for low quenching efficiency to measure the oxygen diffusion coefficient, D.

2. Experimental

2.1. Materials

2.1.1. Modified bentonite

Na-activated bentonite (NaLB) was obtained from bentonite, collected at the bentonite deposits in Lalapaşa- Edirne, Thrace, Turkey (courtesy of Bensan Corp.). The bentonite was treared with 4% (m/m) NaHCO$_3$ solution and dispersed in distillated water at room temperature mixing for 24 h (6 mass% NaLB stock dispersion). pH of the dispersion was 10.7. Benzyl di methyltetradecyl ammonium chloride (BDTDACl) was dissolved in water at 20 mmol/l concentration. 5 ml BDTDACl stock solution, 6.25 ml 6 mass% NaLB stock dispersion and 1.25 ml distillated water were mixed and shaken in order to obtain 3 mass% NaLB+8 mmol/l BDTDACl. This dispersion was shaken overnight and after 24 h the dispersion was diluted to contain 0.0141 g/ml bentonite.

The particle size distributions (PSD) of the bentonite was determined by sedimentation. The particle size was in the range of 50–0.4 μm and average particle size of NaLB was 10 μm. After the modification of clay, the PSD of MNaLB was measured to be in the range of 10–0.4 μm and the average particle size was 1 μm (Table 1). In original NaLB dispersion, 49.8% of the particles were >10 μm, but no particles ≫10 μm were found after addition of BDTDACl (Gunister et al., 2006). Scanning Electron Microscope (SEM) micrographs of the modified bentonite used in this study is seen in Fig. 1. The SEM photographs (Fig. 1) of the modified bentonite were taken after samples were frozen under liquid nitrogen, and then fractured, mounted and coated with gold (300 A°) on an Edwards S 150B sputter coater (Günister et al., 2007).

2.1.2. PS latex

Pyrene labelled polystyrene particles were produced via emulsifier-free radical polymerization. The polymerization reaction was carried out in a 200 ml thermostated round-bottomed four-necked flask, equipped with a glass anchor-shaped stirrer, condenser and nitrogen inlet. Styrene monomer was first introduced in the reactor containing boiled and deionised water and the fluorescent monomer 1-pyrenylmethyl methacrylate (PolyFluor™394) was first dissolved in a small amount of styrene. The potassium persulfate (KPS) as initiator
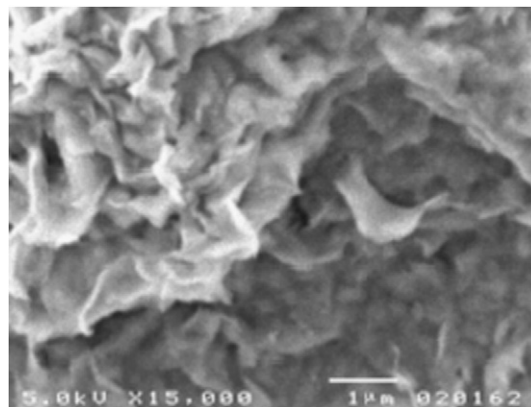

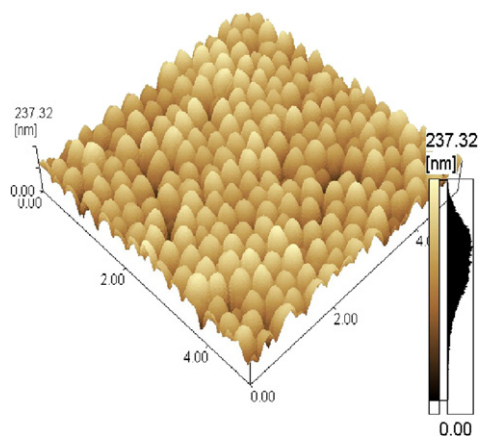**Fig. 1.** SEM microphotograph of MNaLB dispersions (Günister et al., 2007).

Fig. 2. AFM micrograph of PS particles.

Table 2
Experimentally obtained diffusion (D) and mutual diffusion (D_m) coefficients

MNaLB (wt%)	d (μm)	$D \times 10^{-10}$ (cm² s⁻¹)	$k_q \times 10^7$ (M⁻¹ s⁻¹)	$D_m \times 10^{-5}$ (cm² s⁻¹)
0	10.0	7.4 ± 0.13	5.43	18.0 ± 1.24
5	14.6	16.2 ± 1.37	4.08	13.4 ± 2.24
10	12.0	11.9 ± 1.12	7.37	24.5 ± 2.80
20	16.2	29.2 ± 1.29	5.15	17.1 ± 1.06
30	15.1	18.8 ± 0.01	3.79	12.6 ± 0.6
50	15.8	21.8 ± 0.08	6.15	20.4 ± 1.7
60	13.4	26.9 ± 3.96	8.26	27.4 ± 0.93

was dissolved in water and added when the polymerization temperature reached 70 °C. The stirring rate was adjusted to 300 rpm. We used: 100 ml water, 4 g of styrene, 0.1 g of KPS (dissolved in 2 ml water) and 0.0129 g of fluorescent monomer (dissolved in 1 g styrene), and reaction time was 18 h under nitrogen. Fig. 2 shows AFM images of the PS latexes. The particles were spherical and fairly monodisperse, with a mean diameter of 320 nm.

2.2. Film preparation

PS/MNaLB composite films were prepared by casting aqueous dispersions. Distilled water was used to disperse the used materials. Films with 0, 5, 10, 20, 30, 50 and 60 mass% MNaLB content were prepared: where W_{MNaLB} and W_{PS} are the weights of MNaLB clay and PS latex, respectively. By placing the same number of drops on a glass plate with the size of 0.8×2.5 cm² and allowing the water to evaporate, dry films were obtained (Fig. 3a). The thickness of the films was determined from the mass and the density of samples and ranged from 10 to 16 μm (Table 2). The film samples were annealed at 200 °C, above T_g of PS (105 °C) for 10 min to complete film formation of PS particles (Fig. 3b).

In fluorescence measurements for oxygen diffusion experiments, films were placed in a round quartz tube saturated with nitrogen, in Perkin Elmer Model LS-50 fluorescence spectrophotometer. Slit widths were kept at 8 nm. P was excited at 345 nm wavelength. In all experiments the intensity at the emission maximum (395 nm) was used for the P intensity (I) measurements. The intensity I of P was monitored against time for each film after the quartz tube was opened to air. All measurements were carried out at room temperature of 20 °C.

3. Theoretical considerations

3.1. Fluorescence quenching by oxygen

When samples containing fluorescent probes are exposed to air or their solutions saturated with oxygen, the fluorescence intensity of
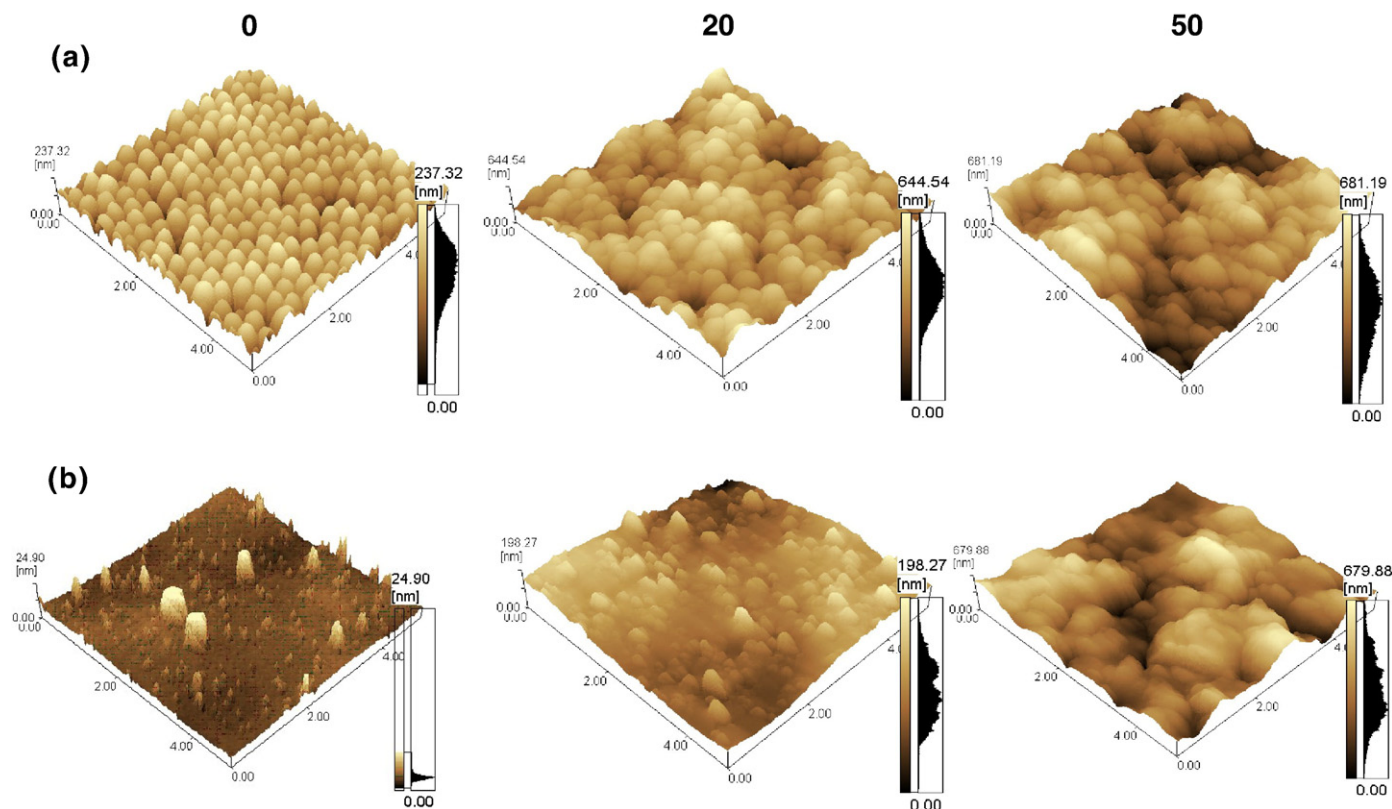
(a)   0   20   50

(b)

Fig. 3. AFM micrographs of composite films prepared with 0, 20 and 50 mass% MNaLB. a– before annealing, b– after annealing at 170 °C for 10 min.
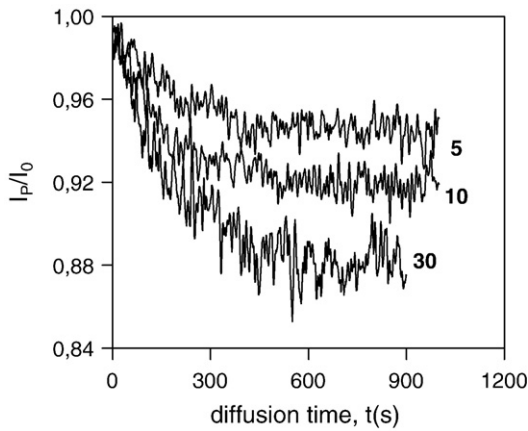
Fig. 4. The time behavior of pyrene, fluorescence intensity, I, during oxygen diffusion into the films. Numbers on each curves indicate the bentonite content (mass%) in the film.

the samples decreases and the rate of fluorescence decay increases due to oxygen quenching of the probe's excited state. The mechanism of quenching involves a sequence of spin-allowed internal conversion processes which takes place within a weakly associated encounter complex between probe and oxygen. The product is either a singlet ground state or an excited triplet species (Birks, 1975).

Data generated from oxygen quenching studies on small molecules in homogeneous solution are usually analyzed using the Stern–Volmer relation, provided that the oxygen concentration $[O_2]$ is not too high (Rice, 1985).

$$\frac{I_0}{I} = 1 + k_q \tau_0 [O_2] \tag{1}$$

In this equation, I and I_0 are the fluorescence intensities in the presence and absence of oxygen, respectively, k_q is the bimolecular quenching rate constant and τ_0 is the fluorescence lifetime in the absence of O_2. This equation requires that the decay of fluorescence is exponential and, that quenching interactions occur with a unique rate constant k_q. From the slope of a plot of I_0/I versus $[O_2]$, k_q can be determined provided that τ_0 is known. Diffusion coefficients related to the quenching events can be calculated from the time-independent Smoluchowski–Einstein (Rice, 1985) equation, $k_0 = 4\pi N_A (D_P + D_q)/1000$. Here, k_0 is the diffusion-controlled bimolecular rate constant and is related to the bimolecular quenching rate constant, k_q as;

$$k_q = p k_0 = \frac{4\pi N_A (D_P + D_q) p R}{1000} \tag{2}$$

where D_P and D_q are diffusion coefficients of the excited probe and quencher, respectively, p is the quenching probability per collision, R is the sum of the collision radii $(R_P + R_q)$, and N_A is the Avogadro number. Eqs. (1) and (2) can also be applied to the case of quenching of polymer-bound excited states in glass as long as the fluorescence decay is exponential and k_q is a unique constant. A simplifying factor in the interpretation of k_q is the general assumption that $D_P \ll D_q$ when the probe is covalently attached to a polymer. For quenchers as small as molecular oxygen, this assumption is reasonable. On the time scale of fluorescence the overall translational diffusion coefficient of the polymer coil is usually not important; the relevant diffusion coefficient is that for motion of individual chain segments.

3.2. Diffusion in plane sheets

When Fick's second law of diffusion is applied to plane sheets and solved by assuming a constant diffusion coefficient, the following

equation is obtained for concentration changes with time (Crank, 1970).

$$\frac{C}{C_0} = \frac{x}{d} + \frac{2}{\pi} \sum_{n=1}^{\infty} \frac{\cos n\pi}{n} \sin \frac{n\pi x}{d} \exp\left(-\frac{D n^2 \pi^2 t}{d^2}\right) \tag{3}$$

where d is the thickness of the slab, D is the diffusion coefficient of the diffusant, and C_0 and C are the concentration of the diffusant at time zero and t, respectively. x corresponds to the distance at which C is measured. We can replace the concentration terms directly with the amount of diffusant by using Eq. (4);

$$M = \int_V C dV \tag{4}$$

when Eq. (3) is considered for a plane volume element and substituted in Eq. (4), the following solution is obtained (Crank, 1970):

$$\frac{M_t}{M_\infty} = 1 - \frac{8}{\pi^2} \sum_{n=0}^{\infty} \frac{1}{(2n+1)^2} \exp\left(-\frac{D(2n+1)^2 \pi^2 t}{d^2}\right) \tag{5}$$

where M_t and M_∞ represent the amounts of diffusant entering the plane sheet at time t and infinity, respectively.

4. Results and discussion

In Fig. 4 pyrene intensity curves are presented against diffusion time for films with different bentonite annealed at 200 °C for 10 min and exposed to oxygen. The emission intensity decreased with time due to the diffusion of oxygen into the film and reached a plateau when the films were saturated. The quenching rate at high bentonite content film was higher than that for low contents indicating rapid diffusion of oxygen molecules into the films with high bentonite content. To interpret this observation Eq. (1) can be expanded in a series for low quenching efficiency i.e. $k_q \tau_0 [O_2] \ll 1$ which leads to

$$I \approx I_0 \left(1 - k_q \tau_0 [O_2]\right) \tag{6}$$

During O_2 diffusion into the films, P molecules are quenched in the domain which is occupied by O_2 molecules at time-t. P intensity at time t can be represented by the volume integration of Eq. (6) as

$$I_t = \frac{\int I dv}{\int dv} = I_0 - \frac{k_q \tau_0 I_0}{V} \int dv [O_2] \tag{7}$$

where dv and V are the differential and total volume of composite film presented in Fig. 5. Performing the integration the following relation is obtained

$$I_t = I_0 \left(1 - k_q \frac{\tau_0}{V} O_2(t)\right) \tag{8}$$

where $O_2(t) = \int dv [O_2]$ is the amount of oxygen molecules diffuse into the latex film at time t. Here $O_2(t)$ corresponds to M_t in Eq. (5).
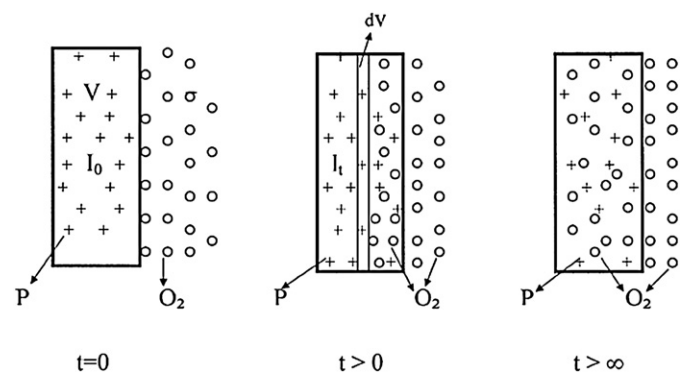

Fig. 5. Cartoon representation of oxygen diffusion into a latex film.

Combining Eq. (5) for $n=0$ for oxygen with Eq. (8) the following useful relation is obtained to interpret the diffusion curves in Fig. 4

$$\frac{I_t}{I_0} = A + \frac{8C}{\pi^2}\exp\left(-\frac{D\pi^2 t}{d^2}\right) \qquad (9)$$

where d is the film thickness and D is the oxygen diffusion coefficient, $C = \frac{k_q \tau_0 O_2(\infty)}{V}$ and $A = 1 - C$. Here $O_2(\infty)$ is the amount of oxygen molecules diffused into latex film at time infinity. The logarithmic form of Eq. (9) can be written a follows:

$$\ln\left(\frac{I_t}{I_0} - A\right) = Ln\left(\frac{8C}{\pi^2}\right) - \frac{D\pi^2}{d^2}t. \qquad (10)$$

Fig. 6a, b and c present $\ln(I_t/I_0 - A)$ versus diffusion time for the latex films at various MNaLB content. Eq. (10) was fitted to these data and C values and diffusion coefficients of oxygen, D were obtained. k_q values were derived from experimentally obtained C values. The total volume of the film, V, was calculated using the surface area of the glass plates (0.8×2.5 cm^2) coated with film and d values given in Table 2. τ_0 was taken as 200 ns (Ugur and Pekcan, 1999). Similar fittings were done for the other film samples and k_q and D values were produced (Table 2). The reproducibility of the results was evaluated by performing five measurements per sample. The deviations from the mean were less than 10 and 15% indicating that D values were quite reproducible. Diffusion coefficients of oxygen, D were strongly dependent on the bentonite content (Fig. 7). The increase of D with increasing bentonite may be attributed to the presence of a large fraction of microvoids inside the films.
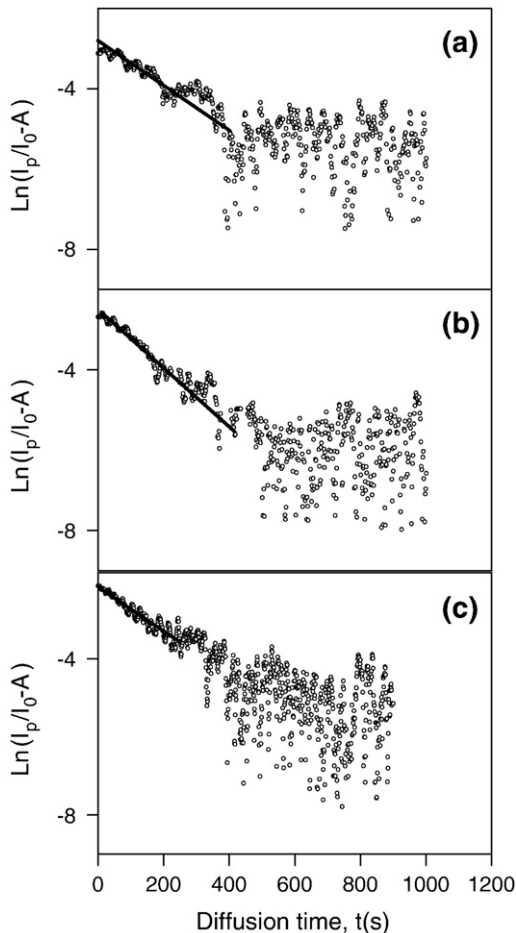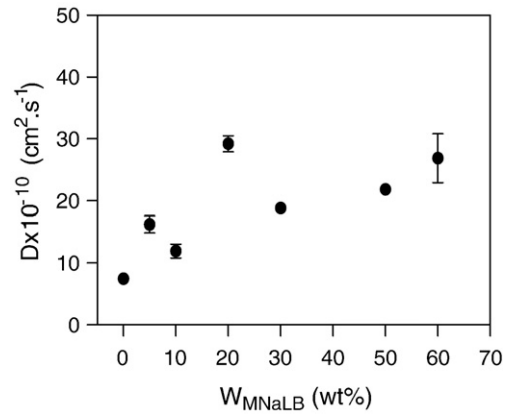

Fig. 7. Plot of the diffusion coefficients, D versus bentonite content in mass.

AFM graphs of the composite films (Fig. 3) also confirm the above picture. After annealing (Fig. 3b) the surface of the pure PS film was smooth indicating that film formation process was completed and PS particles formed a mechanically strong void-free continuous film. The bentonite particles protect some of the PS particles and some particle traces are seen on the surface of the film with 20% bentonite. Despite these traces on the surface, film formation process was almost completed. However, when the amount of bentonite was high (50 mass%), the film formation process could not be completed, i.e., the polymer phase was not continuous. The polymer could no longer fill the gaps between the bentonite particles, and voids were created. These voids enhanced the diffusion rate of oxygen along the film surface.

D values in this study (10^{-10} cm^2 s^{-1}) were one order of magnitude larger than those obtained for pure PMMA films (10^{-11} cm^2 s^{-1}) annealed at various temperatures (Pekcan and Ugur, 1999). This difference shows that the rate of oxygen diffusion in composite films through the voids is much faster than the diffusion rate of oxygen through the continuous polymer matrix. The D values reported here may be compared with those measured in thicker continuous polystyrene films (Bowyer et al., 2004). As film thickness (d) enters the diffusion equation as a quadratic term, both data are in fact comparable.

When the pyrene diffusion in the latex film is omitted and $p=1$ is taken, i.e. $k_q = k_0$ (diffusion-controlled quenching) then Eq. (2) becomes

$$k_q = \frac{4\pi N_A D_m R}{1000} \qquad (11)$$

Here D_m is called "mutual diffusion coefficient" which can be considered the self diffusion coefficient of O_2 in the composite film. If R is the radius of pyrene (Ugur and Pekcan, 1999) in Eq. (11), then the averaged D_m values are found using the known k_q values in Table 2. D_m is independent of the bentonite content i.e. once O_2 penetrates into the film, it moves in short range independent of the material structure. The D_m value obtained in the present study (10^{-5} cm^2 s^{-1}) is one order larger than that previously obtained (10^{-6} cm^2 s^{-1}) using the same technique (Pekcan and Ugur, 1999, 2000). This shows that the voids in composite films promote the rapid quenching of excited pyrene molecules and reduce their response time.

5. Conclusion

The diffusion coefficient of oxygen molecules into composite films was measured by simple SSF technique. The results were consistent with our previous results (Pekcan and Ugur, 1999, 2000). The addition of modified bentonite into the polymer matrix created voids which allowed more rapid diffusion of oxygen. On the other hand, self diffusion of oxygen molecules in the composite films was not affected by the size and the structure of the film, in other words the average value of D_m gave information only on the local environment.

Fig. 6. Logarithmic plots of data in Fig. 4 and their fits to Eq. (10) for a– 5, b– 10 and c– 30 mass%. MNaLB films.

References

Barker, R.E., 1962. Diffusion in polymers: optical techniques. J. Polym. Sci. 58, 553–570.

Bharadwaj, R.K., 2001. Modeling the barrier properties of polymer-layered silicate nanocomposites. Macromolecules 34, 9189–9192.

Birks, J.B., 1975. Organic Molecular Photophysics. Wiley-Interscience, New York.

Bowyer, W.J., Xu, W., Demas, J.N., 2004. Determining oxygen diffusion coefficients in polymer films by lifetimes of luminescent complexes measured in the frequency domain. Anal. Chem. 76, 4374–4378.

Cox, M.E., Dunn, B., 1986a. Oxygen diffusion in poly(dimethyl siloxane) using fluorescence quenching. 1. Measurement technique and analysis. J. Polym. Sci. Part A, Polym. Chem. 24, 621–636.

Cox, M.E., Dunn, B., 1986b. Oxygen diffusion in poly(dimethyl siloxane) using fluorescence quenching. 2. Filled samples. J. Polym. Sci. J. Polym. Sci. Part A, Polym. Chem. 24, 2395–2400.

Crank, J., 1970. The Mathematics of Diffusion. Oxford University Press, London.

Doh, J.G., Cho, I., 1998. Synthesis and properties of polystyrene organoammonium montmorillonite hybrid. Polym. Bull. 41, 511–518.

Friedlander, H.Z., Grink, C.R., 1964. Organized polymerization III. Monomers intercalated in montmorillonite. J. Polym. Sci. Polym. Lett. 2, 475–479.

Gilman, J.W., 1999. Flammability and thermal stability studies of polymer layered-silicate (clay) nanocomposites. Appl. Clay Sci. 15, 31–49.

Gorassi, G., Tortora, M., Vittoria, V., Kaempfer, D., Mülhaupt, R., 2003. Transport properties of organic vapors in nanocomposites of organophilic layered silicate and syndiotactic polypropylene. Polymer 44, 3679–3685.

Gunister, E., Gungor, N., Ece, O.I., 2006. The investigations of influence of BDTDACl and DTABr surfactants on rheologic, electrokinetic and XRD properties of Na-activated bentonite dispersions. Mater. Lett. 60, 666–673.

Günister, E., Unlu, C.H., Atici, O., Ece, O.I., Gungor, N., 2007. Interactions of BDTDACl and DTABr surfactants with montmorillonite in aqueous systems. J. Compos. Mater. 41 (2), 153–164.

Jayarajah, C.N., Yekta, A., Manners, I., Winnik, M.A., 2000. Oxygen diffusion and permeability in alkylaminothionylphosphazene films intended for phosphorescence barometry applications. Macromolecules 33 (15), 5693–5701.

Kato, C., Kuroda, K., Takahara, H., 1981. Preparation and electrical-properties of quaternary ammonium montmorillonite–polystyrene complexes. Clay Clay Miner. 29, 294–298.

Li, Y., Zhao, B., Xie, S.B., Zhang, S., 2003. Synthesis and properties of poly(methyl methacrylate)/montmorillonite (PMMA/MMT) nanocomposites. Polym. Int. 52, 892–898.

Liu, Wu, Q., 2001. PP/clay nanocomposites prepared by grafting–melt intercalation. Polymer 42, 10013–10019.

Lu, C.S., Mai, Y.W., 2005. Influence of aspect ratio on barrier properties of polymer–clay nanocomposites. Phys. Rev. Lett. 95 article number:088303.

Lu, X., Manners, I., Winnik, M.A., 2001a. Polymer/silica composite films as luminescent oxygen sensors. Macromolecules 34, 1917–1927.

Lu, X., Manners, I., Winnik, M.A., 2001b. Fluorescence spectroscopy; new trends. In: Valuer, B., Brochan, J.C. (Eds.), Fluorescence Spectroscopy. Springer Verlag, New York, p. 229. ch. 12.

MacCallum, J.R., Rudkin, A.L., 1978. Novel technique for measuring the diffusion constant of oxygen in polymer-films. Eur. Polym. J. 14, 655–656.

Noh, M.W., Lee, D.C., 1999. Synthesis and characterization of PS–clay nanocomposite by emulsion polymerization. Polym. Bull. 42, 619–626.

Pekcan, O., Ugur, S., 1999. Oxygen diffusion into latex films annealed at various temperatures: a fluorescence study. J. Colloid Interface Sci. 217, 154–159.

Pekcan, O., Ugur, S., 2000. Packing effect on oxygen diffusion in latex films; a photon transmission and fluorescence study. Polymer 41, 7531–7538.

Ray, S.S., Okamoto, M., 2003. Polymer/layered silicate nanocomposites: a review from preparation to processing. Prog. Polym. Sci. 28, 1539–1641.

Rice, S.A., 1985. Diffusion-limited reactions. In: Bamford, C.H., Tipper, C.F.H., Compton, R.G. (Eds.), Comprehensive Chemical Kinetics. Elsevier, Amsterdam.

Ruffolo, R., Evans, C.H., Liu, X., Ni, Y., Pang, Z., Park, P., MacWilliams, A., Gu, X., Lu, X., Yekta, A., Winnik, M.A., Manners, I., 2000. Phosphorescent oxygen sensors utilizing sulfur–nitrogen–phosphorus polymer matrixes: synthesis, characterization, and evaluation of poly(thionylphosphazene)-b-poly(tetrahydrofuran) block copolymers. Anal. Chem. 72, 1894–1904.

Salahuddin, N., Akelah, A., 2002. Synthesis and characterization of poly (styrene-maleic anhydride)–montmorillonite nanocomposite. Polym. Adv. Technol. 13, 339–345.

Shaw, G., 1967. Quenching by oxygen diffusion of phosphorescence emission of aromatic molecules in polymethyl methacrylate. Trans. Faraday Soc. 63, 2181–2189.

Ugur, S., Pekcan, O., 1999. Comparison of dissolution and mutual diffusion coefficients during dissolution of poly(methyl methacrylate) films. Polym. Int. 48, 485–490.

Uğur, Ş., Alemdar, A., Pekcan, Ö., 2005. Films formed from polystyrene latex/clay composites: a fluorescence study. J. Coat. Tech. Res. 2 (7), 565–575.

Uğur, Ş., Alemdar, A., Pekcan, Ö., 2006. The effect of clay particles on film formation from polystyrene latex. Polym. Compos. 27, 299–308.

Vaia, R.A., Jandt, K.D., Kramer, F.J., Giannelis, F.P., 1996. Microstructural evolution of melt intercalated polymer-organically modified layered silicates nanocomposites. Chem. Mater. 8, 2628–2635.

Villaluenga, J.P.G., Khayet, M., Lopez-Manchado, M.A., Valentin, J.L., Seoane, B., Mengual, J.I., 2007. Eu. Polym. J. 43 (4), 1132–1143.